

Cite this: *Chem. Sci.*, 2020, **11**, 6026

All publication charges for this article have been paid for by the Royal Society of Chemistry

Received 28th January 2020  
Accepted 22nd May 2020

DOI: 10.1039/d0sc00505c

rsc.li/chemical-science

## Photo-induced carbocation-enhanced charge transport in single-molecule junctions†

Zhongwu Bei,<sup>b</sup> Yuan Huang,<sup>b</sup> Yangwei Chen,<sup>b</sup> Yiping Cao <sup>\*b</sup> and Jin Li <sup>\*a</sup>

We report the first example of photo-induced carbocation-enhanced charge transport in triphenylmethane junctions using the scanning tunneling microscopy break junction (STM-BJ) technique. The electrical conductance of the carbocation state is enhanced by up to 1.5 orders of magnitude compared to the initial state, with stability lasting for at least 7 days. Moreover, we can achieve light-induced reversible conductance switching with a high ON–OFF ratio in carbocation-based single-molecule junctions. Theoretical calculations reveal that the conductance increase is due to a significant decrease of the HOMO–LUMO gap and also the enhanced transmission close to the Fermi levels when the carbocation forms. Our findings encourage continued research toward developing optoelectronics and carbocation-based devices at the single-molecule level.

### Introduction

Since its inception, molecular electronics has aimed for functional electronic devices using individual molecules.<sup>1</sup> Understanding and investigations of charge transport through single molecules provide critical information for the design of molecular-scale devices.<sup>2–5</sup> Various molecular species are being employed in single-molecule devices for regulating charge transport properties in single-molecule junctions, for instance oligoynes,<sup>6</sup> oligo(phenylene ethynylene),<sup>7</sup> organic radicals,<sup>8</sup> DNA,<sup>9</sup> and peptides.<sup>10</sup> Although carbocations have been widely found in many chemical reactions,<sup>11–13</sup> to date, the applications of carbocation-based molecules as building blocks to fabricate stable and highly conductive molecular devices remain highly challenging due to the intrinsic instability of a majority of carbocations.

On the other hand, an external stimulus for tuning charge transport through molecular junctions also plays a key role in the fabrication of single-molecule devices. Previously several external stimuli such as light,<sup>14</sup> pH,<sup>15</sup> electric fields,<sup>16</sup> mechanical forces,<sup>17</sup> solvents,<sup>18</sup> and electrochemical gates<sup>19</sup> were used to tailor the electronic properties of single-molecule junctions. Among these stimuli, light has an advantage in terms of its remote manner, non-invasiveness, and high spatiotemporal resolution.<sup>20</sup> Therefore the utilization of light to tune charge transport may provide a unique strategy for creating new conceptual molecular devices.

Triphenylmethane leuco derivatives are well-known photochromic molecules, which dissociate into ion pairs under ultraviolet irradiation, producing stable carbocations in the form of triarylmethane dyes and hydroxide ions.<sup>21–23</sup> The stable carbocation dyes have re-emerged as a highly efficient Lewis acid catalysts for a variety of organic transformations. Investigations of this reaction have revealed that the dissociation processes are very fast and proceed with high quantum yields.<sup>22</sup> Such prominent changes in pH have received wide interests as light-induced pH-jump reactions for many applications,<sup>22,23</sup> and also offer potential opportunities to study carbocation-based charge transport properties at the single-molecule level.

In the present work, we selected malachite green leucohydroxide (MGOH) molecules as carbocation emitters to explore laser-induced charge transport in single-molecule junctions. Using the scanning tunneling microscopy break junction (STM-BJ) technique,<sup>24</sup> the single molecule conductance of MGOH and the corresponding junction elongation can be evaluated (Fig. 1a). The dimethylamino moieties at both ends of MGOH serving as the anchoring groups are used to build efficient transport junctions. In the presence of 302 nm UV light, MGOH produces, with high efficiency, malachite green carbocations (MG<sup>+</sup>) and hydroxide ions, thus inducing a minor structural change where the orbital hybridization of the central carbon atom of initial states changes from sp<sup>3</sup> to sp<sup>2</sup>. Such a photo-triggered structural transformation shifts the HOMO–LUMO gap and we demonstrate that the carbocations significantly enhance the conductance and the conductance switching could be highly reversible. The large enhancement in single-molecule conductance suggests that the transport pathway of charges in the carbocation state is markedly different to that of initial states, and it is further supported by the DFT calculations that Breit–Wigner resonance occurs in the carbocation state, leading to a large ON–OFF ratio in the junctions.

<sup>a</sup>Research Center for Analytical Sciences, College of Chemistry, Nankai University, Tianjin 300071, China. E-mail: rengong0225@163.com

<sup>b</sup>Key Laboratory of Optoelectronic Chemical Materials and Devices of Ministry of Education, Jiangnan University, Wuhan 430056, China

† Electronic supplementary information (ESI) available. See DOI: 10.1039/d0sc00505c



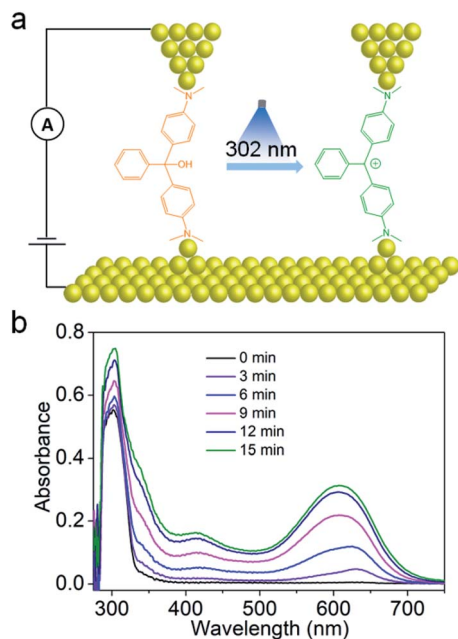


Fig. 1 (a) Schematic of the scanning tunneling microscopy break junction (STM-BJ) setup and photo-induced carbocation forms. MGOH shows the low-conductance state. Upon illumination with 302 nm light, carbocation states were formed and exhibited high conductance. (b) Time-dependent evolution (with 3 min intervals) of the UV-Vis absorption spectra recorded during the reactions from MGOH to  $\text{MG}^+$  upon illumination.

## Results and discussion

To confirm the formation of the carbocations, we performed UV-Vis absorption spectroscopy of MGOH before and after UV illumination as shown in Fig. 1b. Before illumination, MGOH exhibits a single peak at 299 nm. After illumination at 25 °C, two prominent peak bands at 416 nm and 610 nm appeared and their intensities progressively increased with time, which correspond to the characteristic of the triphenylmethane carbocation.<sup>16,18</sup> *In situ* photo-radiation of MGOH results in the orbital hybridization of the central carbon atom changing from  $\text{sp}^3$  to  $\text{sp}^2$ . The formation of the carbocation states is also confirmed by  $^1\text{H-NMR}$  spectra (Fig. S1 in the ESI<sup>†</sup>) and ESI-MS results (Fig. S2 and S3 in the ESI<sup>†</sup>).

To investigate the charge transport properties through the single-molecule carbocation-based junctions, we utilized a home-built STM-BJ technique for trapping single molecules in the mixed solvent of THF and TMB, (1 : 4, v/v) (see the ESI<sup>†</sup> for more details of single-molecule conductance measurements and Fig. S4<sup>†</sup> for the STM-BJ setup and Fig. S5<sup>†</sup> for blank experiment results of the pure solvent). Fig. 2a presents typical conductance–distance traces obtained from MGOH and carbocations. Before illumination, a low conductance at  $\sim 10^{-4.97} G_0$  (0.8 nS) with a plateau length of  $\sim 0.5$  nm is observed, indicating the formation of single-molecule junctions comprising MGOH, where  $G_0$  (equals  $2e^2/h$ , 77.5  $\mu\text{S}$ ) corresponds to the conductance quantum of a single gold–gold atomic junction. After illumination with 302 nm light for 15 min, a higher conductance of  $\sim 10^{-3.43} G_0$  (28.8 nS) with a similar step length is observed.

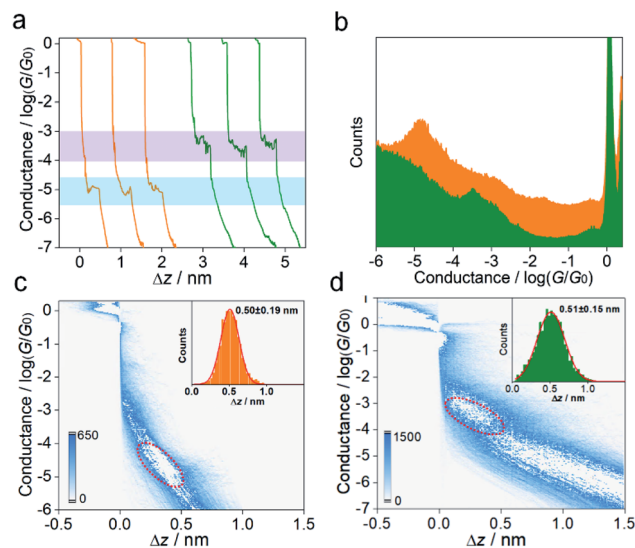


Fig. 2 (a) Typical conductance–distance traces of MGOH (orange) and carbocations (green). (b) 1D conductance–displacement histogram results constructed from thousands of individual traces for MGOH (yellow) and carbocations (green). 2D conductance–displacement histograms versus the plateau relative displacement distributions of MGOH (c) and carbocations (d).

To ensure these features are statistically reproducible, we repeated the measurements thousands of times and compiled the traces into one-dimensional (1D) and two-dimensional (2D) conductance histograms. From the 1D conductance histograms in Fig. 2b, we observed that the molecular conductance peak for MGOH appeared at  $\sim 10^{-4.91} G_0$  (0.9 nS), while the molecular conductance for  $\text{MG}^+$  at  $\sim 10^{-3.40} G_0$  (30.9 nS) is 34 times higher than that of MGOH. The corresponding 2D histograms for MGOH and carbocations are displayed in Fig. 2c and d. Both molecules exhibit distinct molecular plateaus and intensity clouds. The junction elongations for both molecular states show the approximate length of around 0.5 nm (insets of Fig. 2c and d), suggesting the structural change of molecular junctions while the binding configuration of the molecular junctions remained similar. We also calculated the formation probability<sup>25</sup> for both molecular junctions, and the results show that the junction formation probabilities are between 40% and 50% (Fig. S6 in the ESI<sup>†</sup>), indicating that the anchoring ability of both molecule species to Au electrodes is similar.

Control experiments were carried out by measuring the conductance of 4,4'-bis(dimethylamino)triphenylmethane leucohydroxide (LMG). It is found that photo-irradiation of a solution of LMG does not induce any detectable change of conductance within the uncertainty of the measurements (Fig. S7 and S8 in the ESI<sup>†</sup>). These results present unambiguous evidence that the prominent increase of the conductance in triphenylmethane junctions after illumination is ascribable to the photo-induced formation of carbocations. We noted that LMG has a higher conductance compared to MGOH, and the rigorous and fully theoretical explorations on the high-conductance for LMG need further study.



To study the stability of the carbocations, we measured the time-dependent conductance evolution of carbocations in a low-polar solvent (THF/TMB,  $v/v = 1 : 4$ , 0.1 mM) that we used and found it was stable for at least 7 days (Fig. 3a). The ESI-MS results and UV-Vis spectrum further indicate that the material is not completely photo-degraded after 7 days (Fig. S9–S12 in the ESI†). The high stability of  $MG^+$  is probably due to the fact that sulfonated triphenylmethyl carbocations and hydroxide ions form loose ion pairs in a low-polar solvent.<sup>26–28</sup> Previous studies reported that triphenylmethyl carbocations aren't stable and can only exist in water (high-polar) for dozens of minutes.<sup>22,23</sup> To further probe the effect of solvent polarity on carbocation stability, we dissolved MGOH molecules in water (0.1 mM), illuminated it with UV light and measured its single-molecule conductance. It is found that the high conductance states lasted for only 60 min (Fig. 3a) in aqueous solution, which is consistent with previous reports, suggesting the stability of carbocations is affected by solvent polarity. By tuning the solvent polarity, the switching could be designed to be irreversible or reversible. In aqueous solutions, the *in situ* light-induced reactions involving carbocations are reversible and at least three cycles of conductance switching can be achieved as shown in Fig. 3b (Fig. S13 in the ESI†). Carbocation-based junctions in low-polar environments with high stability can serve as conducting interconnects for durable electrical circuits, while carbocation-based junctions with low stability in high-polar environments can act as a light-reversible single-molecule switch. These results suggest carbocations are one of the potential multifunctional building blocks for molecular electronics. Compared with the molecular devices constructed by common molecular systems such as spiropyran<sup>29</sup> and azobenzene,<sup>30</sup> this work based on carbocation molecular species of interest broadens the scope of building blocks in molecular electronics.

To understand the charge transport properties of initial and carbocation states, we turned to density functional theory (DFT) calculations. We first calculated the Au–N binding energies in both molecular junctions and the results show that the Au–N binding energies for MGOH and the carbocations are respectively  $-0.89$  eV and  $-0.41$  eV (see Fig. S14 and S15 in the ESI†),

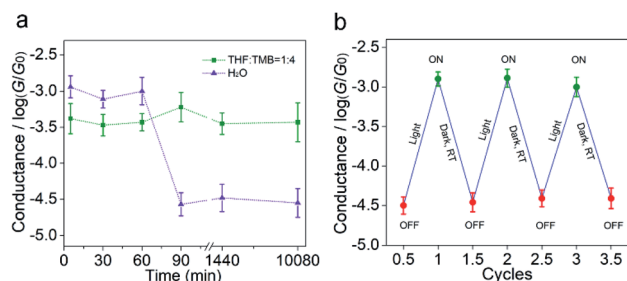


Fig. 3 (a) Measured single-molecule conductance results of the carbocation-based junctions in different solvents with different polarities as a function of time. The green line suggests the long-term stability of the single-molecule conductance of the carbocation states. (b) Reversible switching in conductance of carbocations in aqueous solution.

which imply that dimethylamino moieties in both molecular species can bind to gold electrodes for stable molecular junctions. Next, we calculated their transmission spectra using the non-equilibrium Greens function (NEGF) formalism with DFT.<sup>31–33</sup> Fig. 4a shows the transmission spectra for MGOH and carbocations, which represent the probability that an electron with given energy will transmit through the molecule between the electrodes (see the conformations of both molecules in Fig. S16 in the ESI†). DFT calculations indicate that the HOMO–LUMO gap changes from 4.65 eV for MGOH to 2.59 eV for  $MG^+$  when the carbocation forms (see frontier molecular orbitals and their energy levels in Fig. S17 and Table S1,† and carbocation-based molecular conformations with different counter-ions and different positions and corresponding transmission spectra in Fig. S18 and S19 in the ESI†), which is also confirmed by the red-shift of the UV-Vis spectra in Fig. 1b. Moreover, it is also found that carbocations create a new resonance in the energy level close to Fermi levels ( $E_F$ ), which is responsible for the boosted conductance phenomena through carbocation-based transport junctions. We also note that this resonance in the transmission spectra has a line-shape of the Breit–Wigner distribution.<sup>34–36</sup> The transmission for carbocation states at the Fermi level is more than one order of magnitude higher than that for MGOH, which is in good agreement with the experimental observation. Fig. 4b shows a schematic energy diagram of the position of molecular orbitals of carbocations respective to  $E_F$  of the two electrodes before and after light illumination. Before

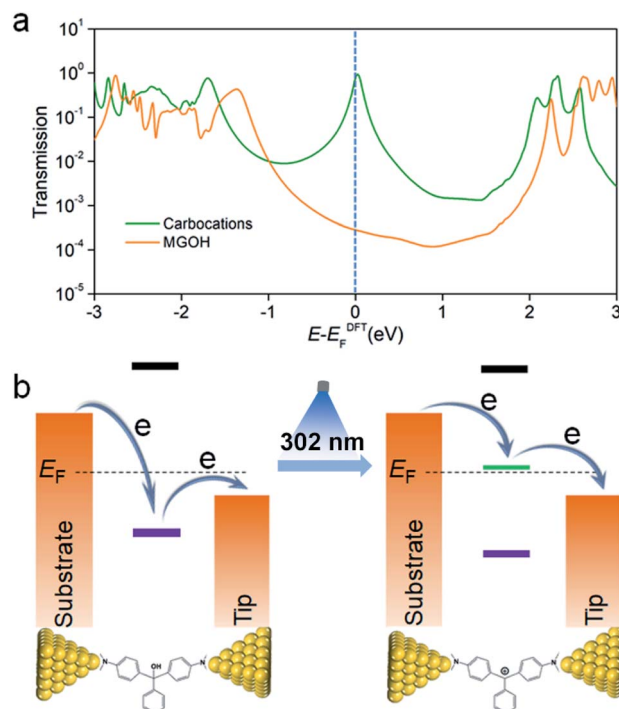


Fig. 4 (a) Transmission as a function of energy for the MGOH (orange) and carbocations (green) at room temperature.  $E_F$  is the Fermi level of the junction based on the DFT calculations. (b) Schematic diagram showing the position of the DFT resonances for carbocations respective to the two electrodes before and after light illumination.



illumination, the energy-level between molecular orbitals of MGOH and  $E_F$  is not aligned, suggesting a large energy barrier in charge transport through the HOMO; while a resonance peak is highly aligned to  $E_F$  in carbocation-based junctions after illumination, which reduces the energy barrier in charge transport and enhances the conductance through LUMO energy lifting. Together, the overall experimental and theoretical studies demonstrate that the *in situ* light-induced approach produces carbocations, which greatly enhance charge transport in triphenylmethane single-molecule junctions.

## Conclusions

In summary, we have demonstrated that carbocations induced by light greatly enhance charge transport in triphenylmethane junctions using the STM-BJ technique. The electrical conductance of the carbocation state is enhanced by up to 1.5 orders of magnitude compared to the initial state and the conductance switching could be reversible. The stable and conductive triphenylmethane carbocations may serve as promising building blocks for future molecular electrical devices. DFT calculations reveal that the conductance increase is due to a significant decrease of the HOMO–LUMO gap and also the enhanced transmission close to the Fermi levels when the carbocation forms. The large conductance enhancement by a light-induced strategy in carbocation-based molecular junctions may be useful for single-molecule optoelectronics and carbocation-based molecular devices.

## Conflicts of interest

There are no conflicts to declare.

## Acknowledgements

We are grateful for financial support from the Guangdong Basic and Applied Basic Research Foundation (2019A1515011182), and the Natural Science Foundation of the Hubei Province (2019CFB582). We also wish to thank Prof. Wenjing Hong from Xiamen University for helping in single-molecule conductance measurements.

## Notes and references

- 1 A. Aviram and M. A. Ratner, *Chem. Phys. Lett.*, 1974, **29**, 277.
- 2 L. Sun, Y. A. Diaz-Fernandez, T. A. Gschneidner, F. Westerlund, S. Lara-Avila and K. Moth-Poulsen, *Chem. Soc. Rev.*, 2014, **43**, 7378.
- 3 Y. Zhang, L. Chen, Z. Zhang, J. Cao, C. Tang, J. Liu, L. Duan, Y. Huo, X. Shao, W. Hong and H. Zhang, *J. Am. Chem. Soc.*, 2018, **140**, 6531.
- 4 J. Zheng, J. Liu, Y. Zhuo, R. Li, X. Jin, Y. Yang, Z.-B. Chen, J. Shi, Z. Xiao, W. Hong and Z.-Q. Tian, *Chem. Sci.*, 2018, **9**, 5033.
- 5 B. Xu and N. J. Tao, *Science*, 2003, **301**, 1221.
- 6 A. Nitzan and M. A. Ratner, *Science*, 2003, **300**, 1384.
- 7 M. T. González, A. Díaz, E. Leary, R. García, M. Á. Herranz, G. Rubio-Bollinger, N. Martín and N. Agrait, *J. Am. Chem. Soc.*, 2013, **135**, 5420.
- 8 J. Liu, X. Zhao, Q. Al-Galiby, X. Huang, J. Zheng, R. Li, C. Huang, Y. Yang, J. Shi, D. Z. Manrique, C. J. Lambert, M. R. Bryce and W. Hong, *Angew. Chem., Int. Ed.*, 2017, **56**, 13061.
- 9 J. C. Genereux and J. K. Barton, *Chem. Rev.*, 2010, **110**, 1642.
- 10 C. Guo, X. Yua, S. Refaely-Abramsoa, L. Sepunaru, T. Bendikov, I. Pecht, L. Kronik, A. Vilan, M. Sheves and D. Cahen, *Proc. Natl. Acad. Sci. U. S. A.*, 2016, **113**, 10785.
- 11 Y. A. Rulev, Z. T. Gugkaeva, A. V. Lokutova, V. I. Maleev, A. S. Peregudov, X. Wu, M. North and Y. N. Belokon, *ChemSusChem*, 2017, **10**, 1152.
- 12 S. S. Bos and F. E. Treloar, *Aust. J. Chem.*, 1978, **31**, 2445.
- 13 R. E. Williams, *Chem. Rev.*, 1992, **92**, 177.
- 14 C. Jia, A. Migliore, N. Xin, S. Huang, J. Wang, Q. Yang, S. Wang, H. Chen, D. Wang, B. Feng, Z. Liu, G. Zhang, D.-H. Qu, H. Tian, M. A. Ratner, H. Q. Xu, A. Nitzan and X. Guo, *Science*, 2016, **352**, 1443.
- 15 Z. Li, M. Smeu, S. Afsari, Y. Xing, M. A. Ratner and E. Borguet, *Angew. Chem., Int. Ed.*, 2014, **53**, 1098.
- 16 F. Schwarz, G. Kastlunger, F. Lissel, C. Egler-Lucas, S. N. Semenov, K. Venkatesan, H. Berke, R. Stadler and E. Lortscher, *Nat. Nanotechnol.*, 2016, **11**, 170.
- 17 I. Franco, C. B. George, G. C. Solomon, G. C. Schatz and M. A. Ratner, *J. Am. Chem. Soc.*, 2011, **133**, 2242.
- 18 D. C. Milan, O. A. Al-Owaedi, M.-C. Oerthel, S. Marqués-González, R. J. Brooke, M. R. Bryce, P. Cea, J. Ferrer, S. J. Higgins, C. J. Lambert, P. J. Low, D. Z. Manrique, S. Martin, R. J. Nichols, W. Schwarzacher and V. M. García-Suárez, *J. Phys. Chem. C*, 2015, **120**, 15666.
- 19 J. Bai, A. Daaoub, S. Sangtarash, X. Li, Y. Tang, Q. Zou, H. Sadeghi, S. Liu, X. Huang, Z. Tan, J. Liu, Y. Yang, J. Shi, G. Meszaros, W. Chen, C. Lambert and W. Hong, *Nat. Mater.*, 2019, **18**, 364.
- 20 S. Cai, W. Deng, F. Huang, L. Chen, C. Tang, W. He, S. Long, R. Li, Z. Tan, J. Liu, J. Shi, Z. Liu, Z. Xiao, D. Zhang and W. Hong, *Angew. Chem., Int. Ed.*, 2019, **58**, 3829.
- 21 C. P. Carvalho, V. D. Uzunova, J. P. Da Silva, W. M. Nau and U. Pischel, *Chem. Commun.*, 2011, **47**, 8793.
- 22 M. Irie, *J. Am. Chem. Soc.*, 1983, **105**, 2078.
- 23 H. Liu, Y. Xu, F. Li, Y. Yang, W. Wang, Y. Song and D. Liu, *Angew. Chem., Int. Ed.*, 2007, **46**, 2515.
- 24 M. T. Gonzalez, A. Diaz, E. Leary, R. Garcia, M. A. Herranz, G. Rubio-Bollinger, N. Martin and N. Agrait, *J. Am. Chem. Soc.*, 2013, **135**, 5420.
- 25 C. Zhan, G. Wang, X. Zhang, Z. Li, J. Wei, Y. Si, Y. Yang, W. Hong and Z. Tian, *Angew. Chem., Int. Ed.*, 2019, **131**, 14676.
- 26 K. Matyjaszewski, C. Lin, A. Bon and J. S. Xiang, *Macromol. Symp.*, 1994, **85**, 65.
- 27 J. P. Richard and W. P. Jencks, *J. Am. Chem. Soc.*, 1982, **104**, 4689.
- 28 X. Creary, E. D. Willis and M. Gagnon, *J. Am. Chem. Soc.*, 2005, **127**, 18114.



- 29 N. Darwish, A. C. Aragonés, T. Darwish, S. Ciampi and I. Diez-Perez, *Nano Lett.*, 2014, **14**, 7064.
- 30 J. M. Mativetsky, G. Pace, M. Elbing, M. A. Rampi, M. Mayor and P. Samori, *J. Am. Chem. Soc.*, 2008, **130**, 9192.
- 31 N. R. Claughton, M. Leadbeater and C. J. Lambert, *J. Phys.: Condens. Matter*, 1995, **7**, 8757.
- 32 J. Taylor, H. Guo and J. Wang, *Phys. Rev. B: Condens. Matter Mater. Phys.*, 2001, **63**, 245407.
- 33 K. Stokbro, J. Taylor, M. Brandbyge and H. Guo, *Ab initio based Non-equilibrium Green's Function Formalism for Calculating Electron Transport in Molecular Devices*, Springer, 2005.
- 34 I. A. Shelykh and N. G. Galkin, *Phys. Rev. B: Condens. Matter Mater. Phys.*, 2004, **70**, 205328.
- 35 C. J. Lambert, *Chem. Soc. Rev.*, 2015, **44**, 875.
- 36 K. Wang, A. Vezzoli, I. M. Grace, M. McLaughlin, R. J. Nichols, B. Xu, C. J. Lambert and S. J. Higgins, *Chem. Sci.*, 2019, **10**, 2396.

